



iJRASET

International Journal For Research in
Applied Science and Engineering Technology



INTERNATIONAL JOURNAL FOR RESEARCH

IN APPLIED SCIENCE & ENGINEERING TECHNOLOGY

Volume: 9 Issue: XII Month of publication: December 2021

DOI: <https://doi.org/10.22214/ijraset.2021.39135>

www.ijraset.com

Call:  08813907089

E-mail ID: ijraset@gmail.com

Spectral and Transmittance Properties of Er^{3+} Doped Zinc Lithium Lead Calcium Borophosphate Glasses

S. L. Meena

Ceramic Laboratory, Department of physics, Jai Narain Vyas University, Jodhpur 342001(Raj.) Ind

Abstract: Zinc lithium lead calcium borophosphate glasses containing Er^{3+} in $(40-x):\text{P}_2\text{O}_5:10\text{ZnO}:10\text{Li}_2\text{O}:10\text{PbO}:10\text{CaO}:20\text{B}_2\text{O}_3:x\text{Er}_2\text{O}_3$ (where $x=1, 1.5, 2$ mol %) have been prepared by melt-quenching method. The amorphous nature of the glasses was confirmed by x-ray diffraction studies. Optical absorption, Excitation, fluorescence and Transmittance spectra were recorded at room temperature for all glass samples. Judd-Ofelt intensity parameters Ω_λ ($\lambda=2, 4, 6$) are evaluated from the intensities of various absorption bands of optical absorption spectra. Using these intensity parameters various radiative properties like spontaneous emission probability, branching ratio, radiative life time and stimulated emission cross-section of various emission lines have been evaluated.

Keywords: ZLLCBP Glasses, Optical Properties, Judd-Ofelt Theory, Transmittance Properties.

I. INTRODUCTION

Rare-earth ions-doped luminescent materials have wide range of applications in which white light emitting diodes, solar cells, lasers, infrared to visible up-converters and optical communications. Oxide glasses are the most stable host matrices for practical applications due to their high chemical durability and thermal stability [1-8]. Among these hosts, the borophosphate system is attractive due to its superior physical, structural and optical properties compared to pure phosphate or borate system [9-13]. The low nonlinear dispersion of the highly rare-earth doped phosphate glasses enables their use in high power applications. Modification of phosphate glass with ZnO had improved glass durability while maintaining low glass transition temperature. Addition of borate in to phosphate glass also increase its durability and created a well-known glass system, namely borophosphate glass. The addition of PbO to the phosphate glass is predictable to increase the glass stability versus devitrification and the glass becomes chemically inactive, due to the capability of PbO to turn as a modifier with structure units PbO_6 [14,15]. Among different rare-earth ions, the Er^{3+} ion has been identified as the most efficient ion for obtaining the lasing action, frequency up-conversion and optical fiber amplification [16-20]. The present work reports on the preparation and characterization of rare earth doped heavy metal oxide (HMO) glass systems for lasing materials. I have studied on the absorption, emission and Transmittance properties of Er^{3+} doped zinc lithium lead calcium borophosphate glasses. The intensities of the transitions for the rare earth ions have been estimated successfully using the Judd-Ofelt theory. The laser parameters such as radiative probabilities(A), branching ratio (β), radiative life time(τ_R) and stimulated emission cross section(σ_p) are evaluated using J.O.intensity parameters(Ω_λ , $\lambda=2, 4$ and 6).

II. EXPERIMENTAL TECHNIQUES

A. Preparation of Glasses

The following Er^{3+} doped zinc lithium lead calcium borophosphate glass samples $(40-x):\text{P}_2\text{O}_5:10\text{ZnO}:10\text{Li}_2\text{O}:10\text{PbO}:10\text{CaO}:20\text{B}_2\text{O}_3: x\text{Er}_2\text{O}_3$ (where $x=1, 1.5, 2$) have been prepared by melt-quenching method. Analytical reagent grade chemical used in the present study consist of P_2O_5 , ZnO, Li_2O , PbO, CaO, B_2O_3 and Er_2O_3 . All weighed chemicals were powdered by using an Agate pestle mortar and mixed thoroughly before each batch (10g) was melted in alumina crucibles in silicon carbide based an electrical furnace.

Silicon Carbide Muffle furnace was heated to working temperature of 1050°C , for preparation of zinc lithium lead calcium borophosphate glasses, for two hours to ensure the melt to be free from gases. The melt was stirred several times to ensure homogeneity. For quenching, the melt was quickly poured on the steel plate & was immediately inserted in the muffle furnace for annealing. The steel plate was preheated to 100°C . While pouring; the temperature of crucible was also maintained to prevent crystallization. And annealed at temperature of 350°C for 2h to remove thermal strains and stresses. Every time fine powder of cerium oxide was used for polishing the samples. The glass samples so prepared were of good optical quality and were transparent. The chemical compositions of the glasses with the name of samples are summarized in Table 1

Table 1 Chemical composition of the glasses

Sample	Glass composition (mol %)
ZLLCBP (UD)	40P ₂ O ₅ :10ZnO:10Li ₂ O:10PbO:10CaO:20B ₂ O ₃
ZLLCBP (ER 1)	39P ₂ O ₅ :10ZnO:10Li ₂ O:10PbO:10CaO:20B ₂ O ₃ :1 Er ₂ O ₃
ZLLCBP (ER 1.5)	38.5P ₂ O ₅ :10ZnO:10Li ₂ O:10PbO:10CaO:20B ₂ O ₃ : 1.5 Er ₂ O ₃
ZLLCBP (ER 2)	38P ₂ O ₅ :10ZnO:10Li ₂ O:10PbO:10CaO:20B ₂ O ₃ : 2 Er ₂ O ₃

ZLLCBP (UD)—Represents undoped zinc lithium lead calcium borophosphate glass specimen.

ZLLCBP (ER) -Represents Er³⁺ doped zinc lithium lead calcium borophosphate glass specimens.

III. THEORY

A. Oscillator Strength

The intensity of spectral lines are expressed in terms of oscillator strengths using the relation [21].

$$f_{\text{expt.}} = 4.318 \times 10^{-9} \int \epsilon(\nu) d\nu \quad (1)$$

where, $\epsilon(\nu)$ is molar absorption coefficient at a given energy ν (cm⁻¹), to be evaluated from Beer–Lambert law.

Under Gaussian Approximation, using Beer–Lambert law, the observed oscillator strengths of the absorption bands have been experimentally calculated, using the modified relation [22].

$$P_m = 4.6 \times 10^{-9} \times \frac{1}{cl} \log \frac{I_0}{I} \times \Delta\nu_{1/2} \quad (2)$$

where c is the molar concentration of the absorbing ion per unit volume, l is the optical path length, $\log I_0/I$ is absorptivity or optical density and $\Delta\nu_{1/2}$ is half band width.

B. Judd-Ofelt Intensity Parameters

According to Judd [23] and Ofelt [24] theory, independently derived expression for the oscillator strength of the induced forced electric dipole transitions between an initial J manifold $|4f^N(S, L) J\rangle$ level and the terminal J' manifold $|4f^N(S', L') J'\rangle$ is given by:

$$\frac{8\pi^2 m c \bar{\nu}}{3h(2J+1)n} \left[\frac{(n^2+2)^2}{9} \right] \times S(J, J') \quad \text{where,} \quad (3)$$

the line strength $S(J, J')$ is given by the equation

$$S(J, J') = e^2 \sum_{\lambda=2, 4, 6} \Omega_{\lambda} \langle 4f^N(S, L) J \| U^{(\lambda)} \| 4f^N(S', L') J' \rangle^2 \quad (4)$$

In the above equation m is the mass of an electron, c is the velocity of light, ν is the wave number of the transition, h is Planck's constant, n is the refractive index, J and J' are the total angular momentum of the initial and final level respectively, Ω_{λ} ($\lambda = 2, 4$ and 6) are known as Judd-Ofelt intensity parameters.

C. Radiative Properties

The Ω_λ parameters obtained using the absorption spectral results have been used to predict radiative properties such as spontaneous emission probability (A) and radiative life time (τ_R), and laser parameters like fluorescence branching ratio (β_R) and stimulated emission cross section (σ_p).

The spontaneous emission probability from initial manifold $|4f^N(S', L') J' \rangle$ to a final manifold $|4f^N(S, L) J \rangle$ is given by:

$$A[(S', L') J'; (S, L) J] = \frac{64 \pi^2 \nu^3}{3h(2J'+1)} \left[\frac{n(n^2+2)^2}{9} \right] \times S(J', J) \quad (5)$$

Where, $S(J', J) = e^2 [\Omega_2 \| U^{(2)} \|^2 + \Omega_4 \| U^{(4)} \|^2 + \Omega_6 \| U^{(6)} \|^2]$

The fluorescence branching ratio for the transitions originating from a specific initial manifold $|4f^N(S', L') J' \rangle$ to a final manifold $|4f^N(S, L) J \rangle$ is given by

$$\beta[(S', L') J'; (S, L) J] = \sum_{S L J} \frac{A[(S', L') J'; (S, L) J]}{A[(S', L') J'; (S, L) J]} \quad (6)$$

where, the sum is over all terminal manifolds.

The radiative life time is given by

$$\tau_{rad} = \sum_{S L J} A[(S', L') J'; (S, L) J] = A_{Total}^{-1} \quad (7)$$

where, the sum is over all possible terminal manifolds. The stimulated emission cross-section for a transition from an initial manifold $|4f^N(S', L') J' \rangle$ to a final manifold $|4f^N(S, L) J \rangle$ is expressed as

$$\sigma_p(\lambda_p) = \left[\frac{\lambda_p^4}{8\pi c n^2 \Delta \lambda_{eff}} \right] \times A[(S', L') J'; (\bar{S}, \bar{L}) \bar{J}] \quad (8)$$

where, λ_p the peak fluorescence wavelength of the emission band and $\Delta \lambda_{eff}$ is the effective fluorescence line width.

D. Nephelauxetic Ratio (β') and Bonding Parameter ($b^{1/2}$)

The nature of the R-O bond is known by the Nephelauxetic Ratio (β') and Bonding Parameters ($b^{1/2}$), which are computed by using following formulae [25, 26]. The Nephelauxetic Ratio is given by

$$\beta' = \frac{\nu_g}{\nu_a} \quad (9)$$

where, ν_a and ν_g refer to the energies of the corresponding transition in the glass and free ion, respectively. The value of bonding parameter ($b^{1/2}$) is given by

$$b^{1/2} = \left[\frac{1-\beta'}{2} \right]^{1/2} \quad (10)$$

IV. RESULT AND DISCUSSION

A. XRD Measurement

Figure 1 presents the XRD pattern of the samples containing show no sharp Bragg's peak, but only a broad diffuse hump around low angle region. This is the clear indication of amorphous nature with in the resolution limit of XRD instrument.

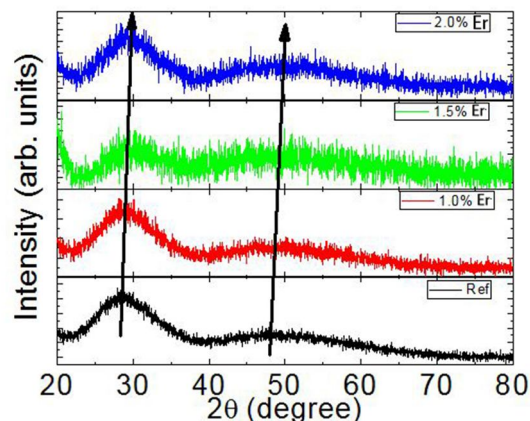


Fig.1: X-ray diffraction pattern of ZLLCBP (ER) glasses.

B. Transmittance Spectrum

The Transmittance spectrum of Er^{3+} doped in zinc lithium lead calcium borophosphate glass is shown in Figure 2.

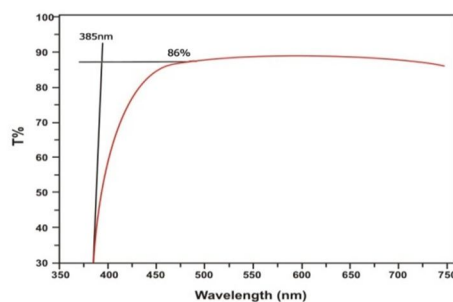


Fig. (2) Transmittance spectrum ZLLCBP ER (01) glass.

C. Absorption Spectra

The absorption spectra of ZLLCBP ER (01) glass, consists of absorption bands corresponding to the absorptions from the ground state $^4\text{I}_{15/2}$ of Er^{3+} ions. Ten absorption bands have been observed from the ground state $^4\text{I}_{15/2}$ to excited states $^4\text{I}_{11/2}$, $^4\text{I}_{9/2}$, $^4\text{F}_{9/2}$, $^4\text{S}_{3/2}$, $^2\text{H}_{11/2}$, $^4\text{F}_{7/2}$, $^4\text{F}_{5/2}$, $^4\text{F}_{3/2}$, $^2\text{H}_{9/2}$ and $^4\text{G}_{11/2}$ for Er^{3+} doped ZLLCBP ER (01) glass.

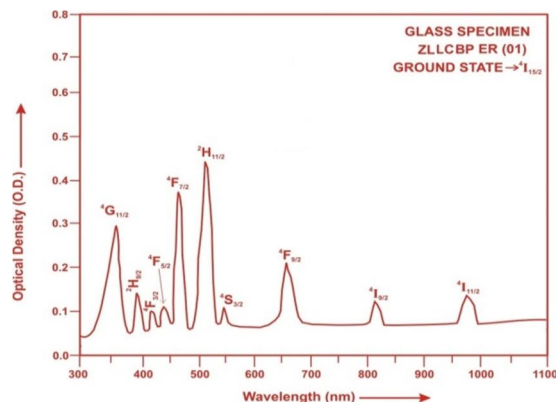


Fig.3: Absorption spectra of ZLLCBP ER (01) glass.

The experimental and calculated oscillator strengths for Er^{3+} ions in zinc lithium lead calcium borophosphate glasses are given in Table 2

Table 2. Measured and calculated oscillator strength ($P^m \times 10^{-6}$) of Er^{3+} ions in ZLLCBP glasses.

Energy level $^4I_{15/2}$	Glass ZLLCBP (ER01)		Glass ZLLCBP (ER1.5)		Glass ZLLCBP (ER02)	
	$P_{\text{exp.}}$	$P_{\text{cal.}}$	$P_{\text{exp.}}$	$P_{\text{cal.}}$	$P_{\text{exp.}}$	$P_{\text{cal.}}$
$^4I_{11/2}$	0.85	0.75	0.82	0.75	0.79	0.75
$^4I_{9/2}$	0.47	0.15	0.42	0.15	0.40	0.15
$^4F_{9/2}$	2.48	1.60	2.44	1.59	2.41	1.59
$^4S_{3/2}$	0.35	0.68	0.31	0.69	0.27	0.68
$^2H_{11/2}$	6.45	2.37	6.42	2.37	6.39	2.38
$^4F_{7/2}$	5.65	2.36	5.62	2.38	5.58	2.36
$^4F_{5/2}$	0.65	0.86	0.61	0.87	0.57	0.87
$^4F_{3/2}$	0.31	0.53	0.26	0.54	0.23	0.53
$^2H_{9/2}$	1.66	1.01	1.61	1.02	1.59	0.99
$^4G_{11/2}$	4.88	6.94	4.81	6.95	4.78	6.95
R.m.s.deviation	1.8233		1.8147		1.80625	

The various energy interaction parameters like Slater-Condon parameters F_k ($k=2, 4, 6$), Lande' parameter ξ_{4f} and Racah parameters E^k ($k=1, 2, 3$) have been computed using partial regression method. The ratio of Racah parameters E^1/E^3 and E^2/E^3 are about 10.35 and 0.049 respectively. Computed values of Slater-Condon, Lande', Racah, nephelauxetic ratio and bonding parameter for Er^{3+} doped ZLLCBP glass specimens are given in Table 3.

Table3. Computed values of Slater-Condon, Lande', Racah, nephelauxetic ratio and bonding parameter for Er^{3+} doped ZLLCBP glass specimens.

Parameter	Free ion	ZLLCBP ER01	ZLLCBP ER1.5	ZLLCBP ER02
$F_2(\text{cm}^{-1})$	441.680	433.918	433.907	433.904
$F_4(\text{cm}^{-1})$	68.327	67.045	67.048	67.046
$F_6(\text{cm}^{-1})$	7.490	7.042	7.043	7.041
$\xi_{4f}(\text{cm}^{-1})$	2369.400	2414.744	2414.726	2414.774
$E^1(\text{cm}^{-1})$	6855.300	6662.232	6662.304	6661.928
$E^2(\text{cm}^{-1})$	32.126	31.342	31.340	31.339
$E^3(\text{cm}^{-1})$	645.570	643.678	643.652	643.686
F_4/F_2	0.15470	0.15451	0.15452	0.15452
F_6/F_2	0.01696	0.016229	0.016231	0.016227
E^1/E^3	10.61899	10.350263	10.351	10.350
E^2/E^3	0.049764	0.04869185	0.048691	0.048687
β'		0.9956098	0.9956340	0.9955572
$b^{1/2}$		0.04685173	0.0467231	0.04713154

Judd-Ofelt intensity parameters Ω_λ ($\lambda = 2, 4$ and 6) were calculated by using the fitting approximation of the experimental oscillator strengths to the calculated oscillator strengths with respect to their electric dipole contributions. In the present case the three Ω_λ parameters follow the trend $\Omega_4 < \Omega_2 < \Omega_6$.

The values of Judd-Ofelt intensity parameters are given in **Table 4**.

Table 4. Judd-Ofelt intensity parameters for Er^{3+} doped ZLLCBP glass specimens.

Glass Specimen	$\Omega_2(\text{pm}^2)$	$\Omega_4(\text{pm}^2)$	$\Omega_6(\text{pm}^2)$	Ω_4/Ω_6
ZLLCBP (ER01)	0.7524	0.3016	0.9877	0.305
ZLLCBP (ER1.5)	0.7605	0.2876	0.9975	0.288
ZLLCBP (ER02)	0.7618	0.2890	0.9899	0.292

D. Excitation Spectrum

The Excitation spectra of Er^{3+} doped ZLLCBP glass specimens have been presented in Figure 4 in terms of Excitation Intensity versus wavelength. The excitation spectrum was recorded in the spectral region 300–600 nm fluorescence at 550nm having different excitation band centered at 350,365, 381, 425, 450, 470and 515 nm are attributed to the $^2\text{K}_{15/2}$, $^4\text{G}_{9/2}$, $^4\text{G}_{11/2}$, $^2\text{G}_{9/2}$, $^4\text{F}_{3/2}$, $^4\text{F}_{5/2}$ and $^2\text{H}_{11/2}$ transitions, respectively. The highest absorption level is $^4\text{G}_{11/2}$ and is at 381nm. So this is to be chosen for excitation wavelength.

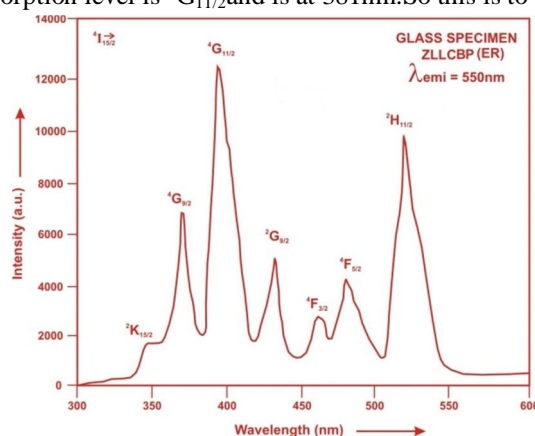


Fig.4: Excitation spectrum of ZLLCBP ER (01) glass.

E. Fluorescence Spectrum

The fluorescence spectrum of Er^{3+} doped in zinc lithium lead calcium borophosphate glass is shown in Figure 5. There are six broad bands ($^4\text{F}_{7/2} \rightarrow ^4\text{I}_{15/2}$), ($^2\text{H}_{11/2} \rightarrow ^4\text{I}_{15/2}$), ($^4\text{S}_{3/2} \rightarrow ^4\text{I}_{15/2}$), ($^4\text{F}_{9/2} \rightarrow ^4\text{I}_{15/2}$), ($^4\text{I}_{11/2} \rightarrow ^4\text{I}_{15/2}$) and ($^4\text{I}_{13/2} \rightarrow ^4\text{I}_{15/2}$) respectively for glass specimens.

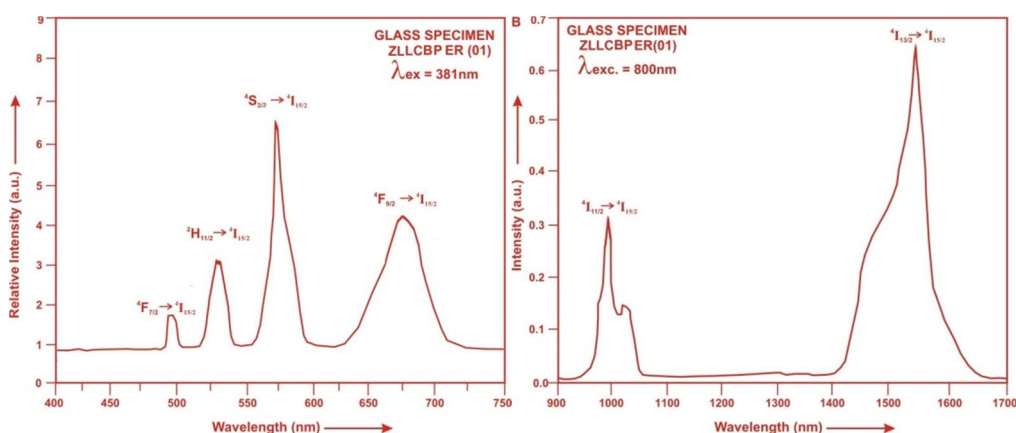


Fig.5: Fluorescence spectrum of ZLLCBP ER (01) glass.

Table 5. Emission peak wave lengths (λ_p), radiative transition probability (A_{rad}), branching ratio (β_R), stimulated emission crosssection (σ_p), and radiative life time (τ) for various transitions in Er^{3+} doped ZLLCBP glasses.

Transition	λ_{max} (nm)	ZLLCBP ER 01				ZLLCBP ER 1.5				ZLLCBP ER 02			
		$A_{rad}(s^{-1})$	β	σ_p (10^{-20} cm^2)	$\tau_R(\mu s)$	$A_{rad}(s^{-1})$	β	$\sigma_p(10^{-20}$ cm^2)	$\tau_R(\mu s)$	$A_{rad}(s^{-1})$	β	σ_p (10^{-20} cm^2)	τ_R (10^{-20} cm^2)
$^4F_{7/2} \rightarrow ^4I_{15/2}$	485	2471.07	0.4203	0.5988	170.07	2491.04	0.4209	0.5861	168.99	2478.91	0.4202	0.5616	169.51
$^2H_{11/2} \rightarrow ^4I_{15/2}$	530	1354.28	0.2303	0.3790		1357.81	0.2294	0.3739		1361.11	0.2307	0.3635	
$^4S_{3/2} \rightarrow ^4I_{15/2}$	550	1097.11	0.1866	0.2917		1110.77	0.1877	0.2910		1104.47	0.1872	0.2819	
$^4F_{9/2} \rightarrow ^4I_{15/2}$	657	729.66	0.1241	0.3442		727.66	0.1230	0.3372		725.79	0.1230	0.3304	
$^4I_{11/2} \rightarrow ^4I_{15/2}$	990	125.73	0.0214	0.3854		127.23	0.0215	0.3840		126.57	0.0215	0.3683	
$^4I_{13/2} \rightarrow ^4I_{15/2}$	1538	102.12	0.0174	1.3517		103.18	0.0174	1.3427		102.65	0.0174	1.2994	

V. CONCLUSION

In the present study, the glass samples of composition $(40-x):P_2O_5:10ZnO:10Li_2O:10PbO:10CaO:20B_2O_3:xEr_2O_3$ (where $x = 1, 1.5, 2$ mol %) have been prepared by melt-quenching method. The value of stimulated emission cross-section (σ_p) is found to be maximum for the transition ($^4I_{13/2} \rightarrow ^4I_{15/2}$) for glass ZLLCBP (ER 01), suggesting that glass ZLLCBP (ER 01) is better compared to the other two glass systems ZLLCBP (ER1.5) and ZLLCBP (ER02).

REFERENCES

- Shoaib, M., Chanthima, N., Rooh, G., Rajaramakrishna, R. and Kaewkhao, J. (2019). Physical and luminescence properties of rare earth doped phosphate glasses for solid state lighting applications. Thai interdisciplinary research, 14, 3, 20 – 26.
- Swapna, K., Mahamuda, S., Venkateswarlu, M., Srinivasa Rao, A., Jayasimhadri, M., Shakya, S. and Prakash, G. V. (2015). Up-conversion and NIR (~1.5 μm) luminescence studies of Er^{3+} doped zinc alumina bismuth borate glasses. J. Lumin. 163, 55-63.
- Wantana, N. (2017). Energy transfer from Gd^{3+} to Sm^{3+} and luminescence characteristics of $CaO-Gd_2O_3-SiO_2-B_2O_3$ scintillating glasses, J. Lumin., 181, 382–386.
- Campbell, J. H. and Suratwala, T. I. (2000). Nd^{3+} -doped phosphate glasses for high-energy/high-peak-power lasers. J. Non-Cryst. Solids, 263, 318–341.
- Gaël, P., Cassanjes, F. C., de Araújo, Cid B., Jerez, Vladimir A., Ribeiro, Sidney J. L., Messaddeq, Y. and Poulain, M. (2003). Optical properties and frequency upconversion fluorescence in a Tm^{3+} -doped alkaliniobium tellurite glass. AIP Journal of Applied Physics 93, 3259.
- Meena, S. L. (2017). Spectroscopic Properties of Eu^{3+} Doped in Yttrium Zinc Lithium Bismuth Borate Glasses. The Int. J. Eng. and Scie. (IJES), 6, 10, 30-36.
- Narayanan, M. K. and Shashikala, H. D. (2015). Thermal and optical properties of $BaO-CaF_2-P_2O_5$ glasses, J. Non-Cryst. Solids, 422, 6-11.
- Reddi Babua, M., Mohan Babua, A. and Rama Moorthy, L. (2018). Structural and optical properties of Nd^{3+} -doped lead borosilicate glasses for broadband laser amplification, International Journal of Applied Engineering Research, 13, 10, 7692-7700.
- Guan, P. X., Yew, E. T., Ming, L. P., Shamsuri, W. N. W. and Hussin, R. (2014). Structural and Luminescence Study of Rare Earth and Transition Metal Ions Doped Lead Zinc Borophosphate Glasses, Adv. Mat. Res. 895, 280-283.
- Rohaizad, A., Hussin, R., Aziz, N. A. S., Uning, R. and Bohari, N. Z. I. (2013). Vibrational Studies of Zinc Antimony Borophosphate Glasses Doped Rare Earth, J. Tek. (Sci. and Eng.), 62(3), 119-122.
- Kumar, G. R. and Rao, C. S. (2020). Influence of Bi_2O_3 , Sb_2O_3 and Y_2O_3 on optical properties of Er_2O_3 -doped $CaO-P_2O_5-B_2O_3$ glasses, Bull. Mater. Sci. 43:71, 1-7.
- Pang, X. G., Eue, T. Y., Leong, P. M., Shamsuri, W. N. W. and Hussin, R. (2014). Structural and Luminescence Study of Rare Earth and Transition Metal Ions Doped Lead Zinc Borophosphate Glasses, Adv. Mat. Res., 895, 280-283.
- S. L. Meena (2020). Spectral and Thermal Properties of Ho^{3+} Doped in Zinc Lithium Alumino Antimony Borophosphate Glasses, IJSDR 5 (11), 127-133.
- Salem, S. M. and Mohamed, E. A. (2011). Electrical conductivity and dielectric properties of $Bi_2O_3-GeO_2-PbO-MoO_3$ glasses, J. Non-Cryst. Solids, 357, 1153-1159.
- Reis, S. T., Faria, D., Martinelli, J. R., Pontuschka, W. M., Day, D. E. and Parititi, C. (2002). Structural features of lead iron phosphate glasses, J. Non-Cryst. Solids, 304, 188-194.
- Yannick L., Mohammed El Amradoui, Jefferson L Ferrari, Pier-Luc Fortin, Sidney R. and Youne Messaddeq (2013). Infrared to Visible Up-Conversion Emission in Er^{3+}/Yb^{3+} codoped Fluoro phosphate Glass Ceramics, J. American Ceramic Society 96(3), 825-832.
- Dousti, M. R., Poirier, G. Y. and de Camargo, A. S. S. de, (2020). Tungsten Sodium Phosphate glasses doped with trivalent rare earth ions (Eu^{3+} , Tb^{3+} , Nd^{3+} , Er^{3+}) for visible and near infrared applications, Journal of Non-Crystalline Solids 530, 119838.
- Bosca, M., Pop, L., Borodi, G., Pascuta, P. and Culea, E. (2009). XRD and FTIR structural investigations of Erbium doped Bismuth lead silver glasses and glass ceramics, Journal of Alloys and Compounds.



- [19] Dutebo, M. T. and Shashikala, H.D.(2020). Influence of (Er^{3+} , La^{3+} , Ce^{4+}) additions on physical and optical properties of 50 CaO- 50 P_2O_5 glasses, *Physica B: Condensed Matter* 597, 412358.
- [20] Zhang, J., Wang, N., Guo, Y., Cai, M., Tian, Y., Huang, F. and Xu, S. (2018). Tm^{3+} doped lead silicate glass sensitized by Er^{3+} for efficient $\sim 2 \mu\text{m}$ mid infrared laser material, *Spectrochimica Acta Part A: Molecular and Biomolecular Spectroscopy* 199, 65-70.
- [21] Gorller-Walrand, C. and Binnemans, K. (1988). Spectral Intensities of f-f Transition. In: Gshneidner Jr., K.A. and Eyring, L., Eds., *Handbook on the Physics and Chemistry of Rare Earths*, Vol. 25, Chap. 167, North-Holland, Amsterdam, 101.
- [22] Sharma, Y.K., Surana, S.S.L. and Singh, R.K. (2009). Spectroscopic Investigations and Luminescence Spectra of Sm^{3+} Doped Soda Lime Silicate Glasses. *Journal of Rare Earths*, 27, 773.
- [23] Judd, B.R. (1962). Optical Absorption Intensities of Rare Earth Ions. *Physical Review*, 127, 750.
- [24] Ofelt, G.S. (1962). Intensities of Crystal Spectra of Rare Earth Ions. *The Journal of Chemical Physics*, 37, 511.
- [25] Sinha, S.P. (1983). Systematics and properties of lanthanides, Reidel, Dordrecht.
- [26] Krupke, W.F. (1974). *IEEE J. Quantum Electron* QE, 10, 450.



10.22214/IJRASET



45.98



IMPACT FACTOR:
7.129



IMPACT FACTOR:
7.429



INTERNATIONAL JOURNAL FOR RESEARCH

IN APPLIED SCIENCE & ENGINEERING TECHNOLOGY

Call : 08813907089  (24*7 Support on Whatsapp)